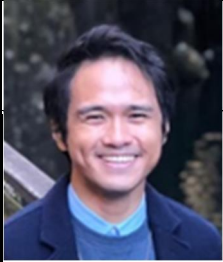


2-3. IROAST Postdoctoral Researchers

No.	Name	Project Title
2-3-1	Jonas Karl Christopher Nuevas AGUTAYA	Elucidation of the gas sensing mechanism of semiconductor metal oxides by a combined DRIFTS and DFT approach
2-3-2	Muhammad Sohail AHMAD	Graphene based materials as membrane reactor the electrocatalytic hydrogenation reaction
2-3-3	Nobleson KUNJAPPY	Characterization of Noise Components in Pulsar Timing Signals for Enhanced Gravitational Wave Detection
2-3-4	Prafulla Bahadur MALLA	Seismic Performance and Evaluation of Hybrid Frame with CFST column continuous Beam Joints
2-3-5	Mohammad Atiqur RAHMAN	Oxide nanosheet as electrolyte for application in fuel cell
2-3-6	Reetu Rani	Applications of Functional Materials in Environmental Remediation

No. 2-3-1	Elucidation of the gas sensing mechanism of semiconductor metal oxides by a combined DRIFTS and DFT approach			
Name	Jonas Karl Christopher Nuevas AGUTAYA	Title	Postdoctoral Researcher	
Affiliation	IROAST Email: jnagutaya@chem.kumamoto-u.ac.jp			
Research Field	Advanced materials			

[Details of activities]

1. Research outline and its perspective

This research employs diffuse reflectance infrared Fourier transform spectroscopy (DRIFTS) to elucidate the gas sensing mechanism of semiconductor metal oxide (SMOX)-based sensors. To complement the experimental results, calculations based on the density functional theory (DFT) are also performed. This study will provide a chemist's perspective in modeling gas sensing for the development of better sensors.

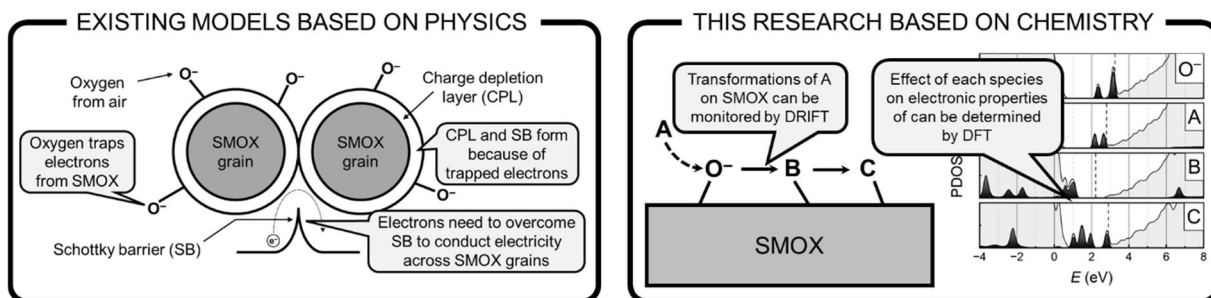


Figure 1. Models for the gas sensing mechanism of SMOX based on physics (existing models) and chemistry (this research)

2. Research progress and results in this fiscal year

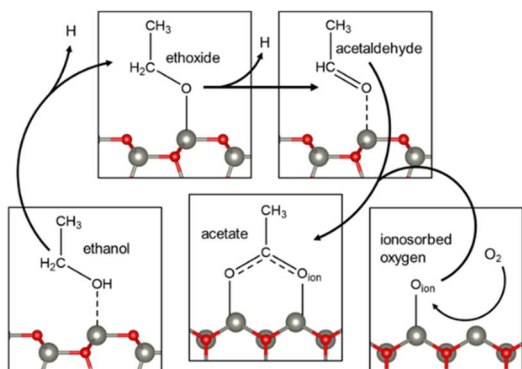


Figure 2. Proposed pathway for the conversion of ethanol over the ZnO (10 $\bar{1}$ 0) surface

[Published] DFT calculations were performed in a study on the ethanol sensing mechanism of ZnO nanorods. Comparing the dimensions of the optimized structure of ZnO with the interatomic distances and angles measured by high-angle annular dark field scanning transmission electron microscopy, the (10-10) plane of ZnO was determined to be the dominant surface in the sensing layer. Using DRIFTS and product gas analyses, the adsorbates and products that were formed from ethanol during its detection were identified. Based on these experimental data, a pathway for the conversion of ethanol over ZnO(10-10) was proposed as shown in Figure 2.

To determine the effect of each adsorbed species on the electronic properties of ZnO, calculations involving projected density of states (PDOS) were also performed. The PDOS plots in Figure 3 show the energy levels introduced by each species in the reaction pathway. In the case of adsorbed oxygen (O_{ion}) and ethoxide, the energy levels within the band gap of ZnO and intersecting the Fermi level (dashed line) indicated an increase in the electrical resistivity of ZnO. In the case of acetaldehyde and acetate, on the other hand, the shift of these energy levels away from the Fermi level and some into the conduction band of ZnO indicated a decrease in its electrical resistivity. From sensor performance measurements, the exposure of the ZnO nanorods to ethanol resulted in a decrease in its electrical resistance. Therefore, the dehydration of ethanol to acetaldehyde and further oxidation of acetate are proposed to be key reactions in the detection of ethanol by the ZnO nanorods.

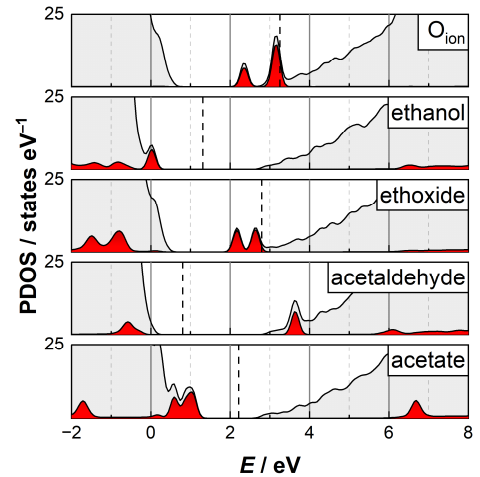


Figure 3. Total density of states (DOS, gray region) and the projected contribution of the adsorbates (PDOS, red region) on ZnO(10-10)

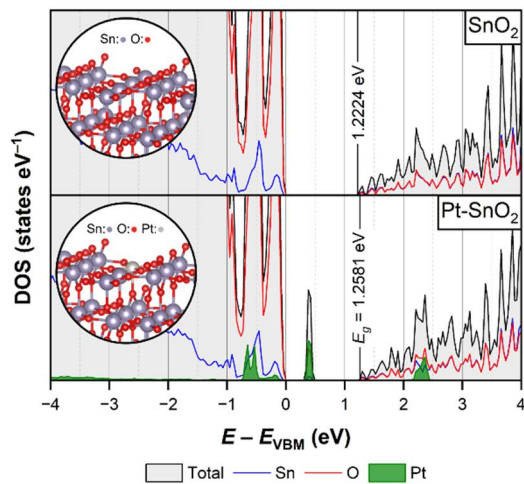


Figure 4. Total density of states (DOS) of SnO_2 and Pt-doped SnO_2 (Pt- SnO_2), and projected contributions of Sn, O, and Pt. Insets: Optimized structures of SnO_2 and Pt- SnO_2

[*On-going*] The combined experimental and theoretical approach was also applied to the elucidation of the ethanol gas sensing mechanism of Pt-doped SnO_2 . In this case, instead of morphological control, the sensitivity of the SnO_2 was improved by doping it with platinum. Characterization of the material using HAADF-STEM showed that both Pt dopants and nanoclusters formed upon the addition of platinum using the liquid-phase method, with the latter feature forming more prominently at higher doping concentrations. DOS calculations revealed that the addition of Pt introduces an energy state within the bandgap of SnO_2 as shown in Figure 4. This energy state effectively increases the electrical resistivity of SnO_2 . Upon the conversion of ethanol on the surface of either SnO_2 or Pt-doped SnO_2 ,

particularly to acetate, there is a decrease in its electrical resistivity as a result of the formation of energy levels in its conduction band, which are associated with the orbitals of acetate. In the case of Pt-doped SnO_2 , this decrease is compounded by the shift in the energy state of Pt previously in its bandgap to its conduction band. Consistent with these findings were the experimental results, which showed that the sensitivity of SnO_2 was improved by doping the material with platinum.

[*Published*] DFT calculations were also performed to determine the effect of formamidinium (FA)-substitution in the photoemission of CsPbI₃ perovskite quantum dots. As shown in Figure 5, the top of the valence band and the bottom of the conduction band are dominated by the energy states of I and Pb, respectively, regardless of the concentration of FA. Therefore, the sites of the electronic transition are primarily I and Pb, indicating that FA, as well as Cs, are mere spectators in the photoactivity of the hybrid Cs_xFA_{1-x}PbI₃ quantum dots. The FA-substitution, however, resulted in a distortion of the cubic structure of CsPbI₃ to a pseudo-orthorhombic structure. In the experiments, the greater resistance of the hybrid Cs_xFA_{1-x}PbI₃ quantum dots to thermal stress and degradation in polar solvents compared to purely inorganic CsPbI₃ quantum dots can be attributed to this pseudo-orthorhombic structure.

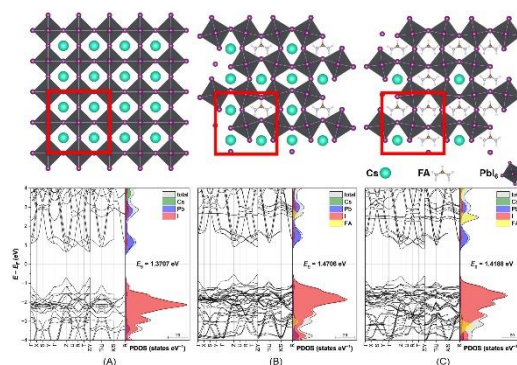


Figure 5. Optimized crystal structures of (A) CsPbI₃, (B) Cs_{0.75}FA_{0.25}PbI₃, and (C) Cs_{0.25}FA_{0.75}PbI₃, and their corresponding band structures and projected density of states. The red rectangle represents the supercell used in the simulations.

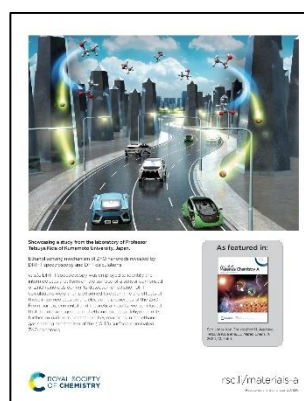
3. List of awards, grants, and patents


- None

4. List of journal papers in international journal as of the end of December 2024

- P. R. Pratama, A. D. Pramata, Y. Suenari, **J. K. C. N. Agutaya**, Y. Nagata, T. Shinkai, Y. Inomata, M. I. P. Hidayat, B. Manna, Y. Akaishi and T. Kida, “Lattice engineering for enhancing the stability of CsPbI₃/Cs_xFA_{1-x}PbI₃ quantum dots synthesized via a direct arrangement”, *Mater. Chem. Front.*, 2025, **9**, 288-298.
- P. R. Pratama, A. D. Pramata, F. Shiga, **J. K. C. N. Agutaya**, Y. Inomata, B. Manna, A. Purniawan, Y. Akaishi and T. Kida, “Green-emitting CsPbI₃ nanorods decorated with CsPb₂I₅ and Cs₄PbI₆ nanoclusters”, *J. Mater. Chem. C*, 2024, **12**, 17611–17619.
- T. Shinkai, **J. K. C. N. Agutaya**, B. Manna, M. Boepple, M. Iwai, K. Masumoto, K. Koga, K. Kawanami, Y. Nakamura, A. T. Quitain, K. Suematsu, Y. Inomata, N. Barsan and T. Kida, “Ethanol sensing mechanism of ZnO nanorods revealed by DRIFT spectroscopy and DFT calculations”, *J. Mater. Chem. A*, 2024, **12**, 7564–7576.

****Featured as the back cover of the issue through the IROAST Publication Support Program**



No. 2-3-2	Graphene based materials as membrane reactor the electrocatalytic hydrogenation reaction			
Name	Muhammad Sohail AHAMD	Title	Postdoctoral Researcher	
Affiliation	IROAST Email: sohail@kumamoto-u.ac.jp			
Research Field	Advanced materials			

Details of activities

1. Research Outline and Perspective

Graphene-based membrane reactors offer a promising platform for electrocatalytic hydrogenation reactions, enabling selective hydrogenation of organic compounds with high efficiency. By incorporating functionalized graphene materials with controlled porosity and catalytic sites, these membranes facilitate enhanced proton transfer and catalytic performance. This research aims to develop novel graphene-based membranes with tunable properties for sustainable hydrogenation applications (Figure 1). The expected impact includes improved reaction selectivity, stability, and energy efficiency for green chemical processes.

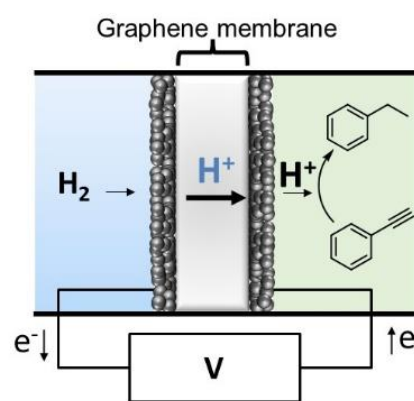
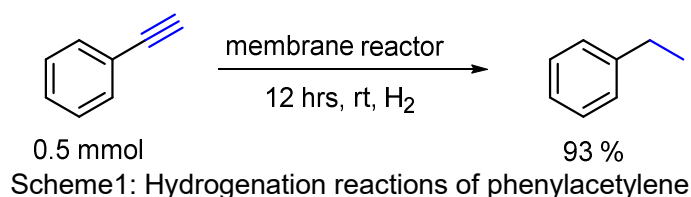


Fig.1: Hydrogenation reactions using membrane.

2. Research Progress and Results in the Fiscal Year

During the fiscal year, significant advancements were made in synthesizing and characterizing functionalized graphene-based membranes. Key activities included:

- Fabrication of graphene oxide (GO) and cerium functionalized GO (Ce-GO) membranes.
- Electrochemical testing of hydrogen permeation and hydrogenation efficiency.
- Structural analysis using XRD, and SEM to confirm membrane integrity and catalytic sites.
- Successful demonstration of selective hydrogenation of organic molecules under mild electrochemical reaction conditions Scheme1.




These findings suggest that the developed membranes enhance hydrogen selectivity and reaction efficiency. The ongoing work focuses on optimizing membrane composition and testing under industrially relevant conditions.

3. Research Plan for the Next Fiscal Year

Building upon the progress, the next fiscal year will focus on:

- Investigating long-term stability and recyclability of the membranes.
- Exploring additional functionalization strategies to improve catalytic performance.
- Extending the scope of the study to a wide range of hydrogenation reactions, including biomass-derived compounds.

This research aims to bridge the gap between fundamental material science and real-world hydrogenation applications, contributing to sustainable and energy-efficient chemical synthesis.

No. 2-3-3	Characterisation of Noise Components in Pulsar Timing Signals for Enhanced Gravitational Wave Detection			
Name	Nobleson KUNJAPPY	Title	Postdoctoral Researcher	
Affiliation	IROAST Email: nobleson@kumamoto-u.ac.jp			
Research Field	Data science and AI			

1. Research outline and its perspective

Detecting low-frequency gravitational waves (GWs) through pulsar timing represents a groundbreaking area at the crossroads of astrophysics and data science. Pulsars are dense neutron stars that emit periodic radio signals that act as precise cosmic clocks. Variations in their timing caused by gravitational waves provide valuable insights into phenomena such as black hole mergers. However, this method faces challenges due to noise within pulsar signals, making it essential to investigate and address these issues to enhance the sensitivity of GW detection.

This research project focuses on systematically identifying and mitigating noise sources in pulsar timing data. By analyzing factors such as intrinsic pulsar timing noise, from the interstellar medium, and instrumental artifacts, the study aims to implement advanced methods to process these signals. These methods will facilitate the removal of noise while preserving gravitational wave signatures, improving the signal-to-noise ratio and ensuring more reliable and confident GW detection through pulsar timing arrays.

2. Research progress and results in the fiscal year

The research progresses through two parallel streams:

1. Data from multiple radio telescopes across different Pulsar Timing Arrays (PTAs) have been combined for a selected sample of pulsars. During this fiscal year, contributions were made to testing a module within the TEMPO2 software package designed for integrating data from various telescopes. This module accounts for differences in fiducial Dispersion Measures (DMs) observed at each telescope, ensuring consistent alignment of Times of Arrival (ToAs) across datasets. By standardizing the ToAs, the module reduces the number of parameters required for noise analysis, significantly decreasing the computational time needed for gravitational wave analysis.
2. During this fiscal year, substantial effort was dedicated to preparing a dataset comprising approximately seven years of observations conducted with the Upgraded Giant Metrewave Radio Telescope (uGMRT). The associated data release paper has been submitted for review, and we are currently addressing reviewer comments.

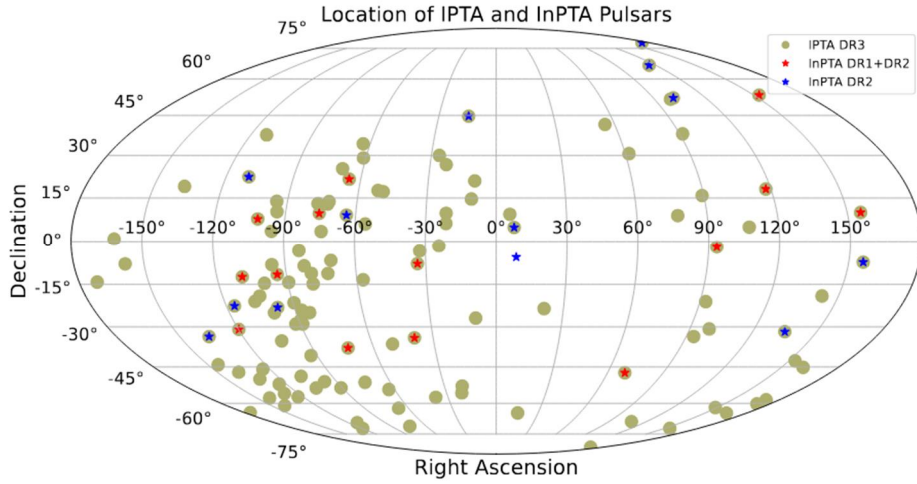


Figure 1. The sky distribution for 27 pulsars included in this data release is shown, marked by red and blue stars, representing observations made with the InPTA experiment between November 2016 and March 2024. 14 pulsars indicated by red stars were part of the InPTA DR1, whereas pulsars marked by blue stars are added in the present data release along with 14 InPTA DR1 pulsars. Green circles indicate pulsars that are planned to be included in the upcoming third data release of IPTA.

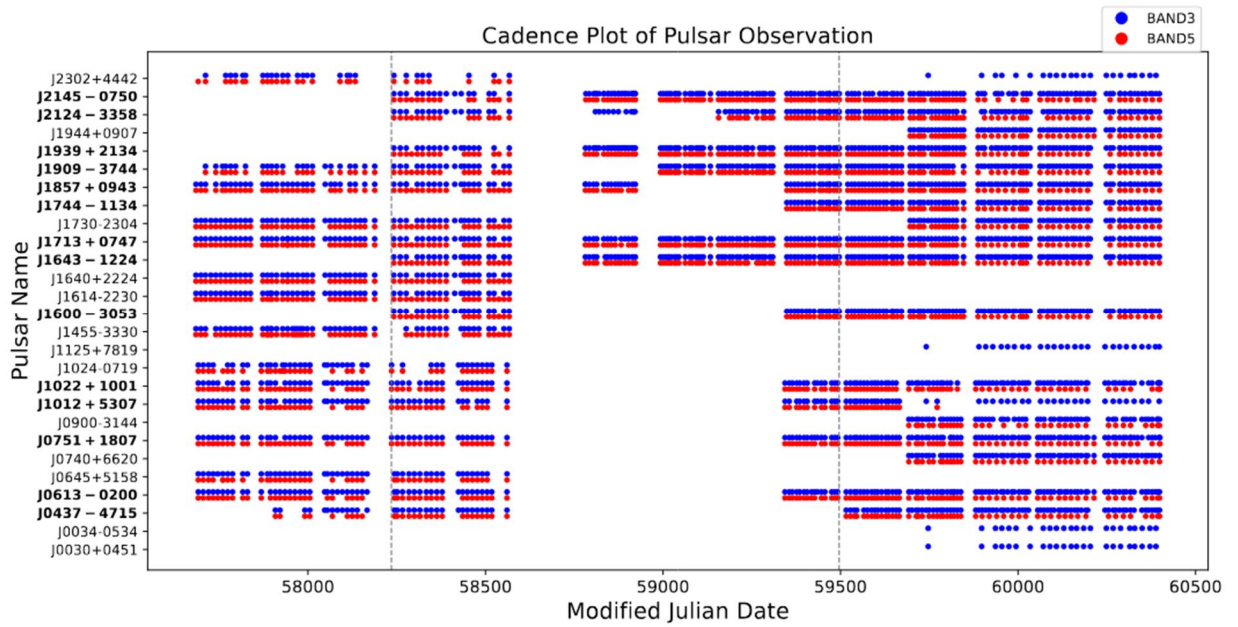


Figure 2: The observation cadence for 27 pulsars included in the present data release is shown across a range of Modified Julian Dates (MJD). Most of these pulsars were observed concurrently in band 3 (blue circles) and band 5 (red circles) of the uGMRT as part of the InPTA experiment. 14 pulsars highlighted in bold were also part of the InPTA DR1 (Tarafdar et al., 2022), and the vertical dashed lines indicate the time span of data that was included in InPTA DR1 for these pulsars.

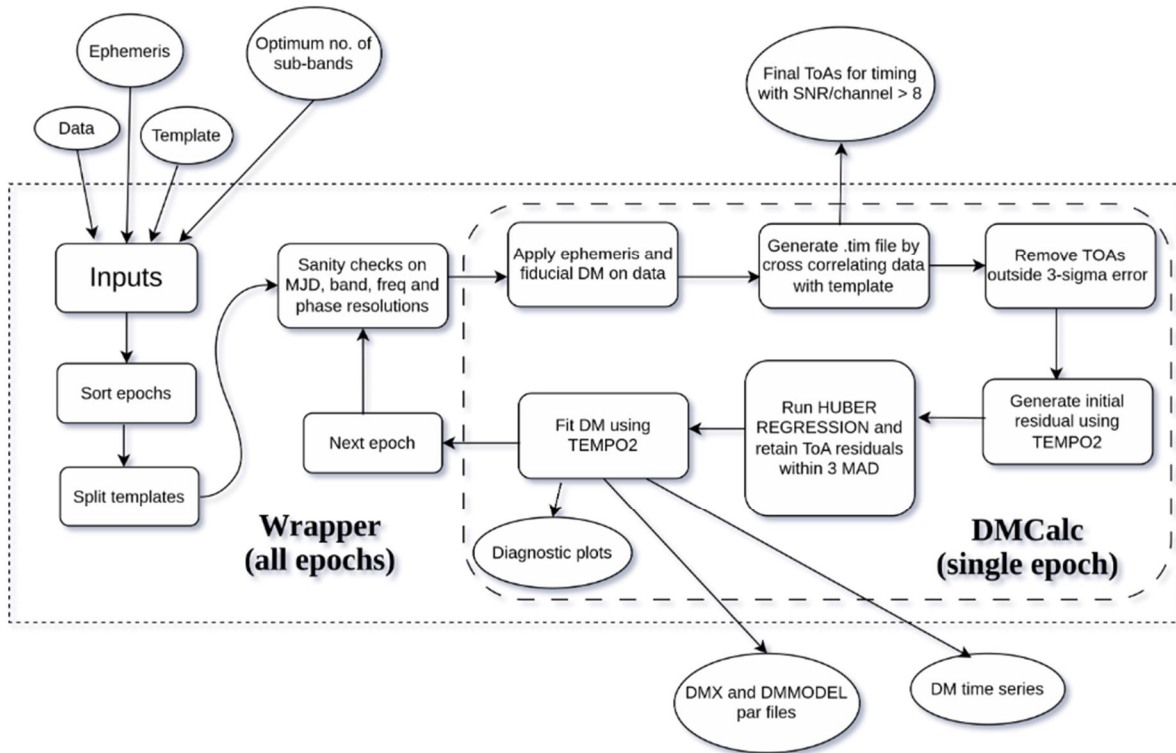
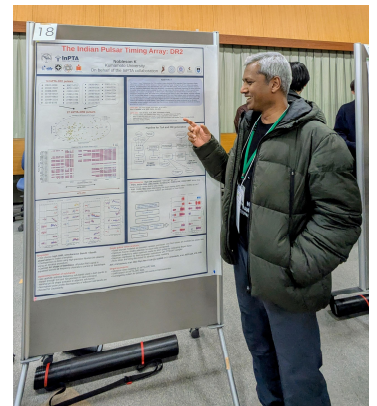


Figure 3: This workflow diagram illustrates the comprehensive process used to estimate ToA and DM using DMCalc and the wrapper script. The wrapper applies the DMCalc processing steps across all epochs, performing essential sanity checks. For each epoch, DMCalc fits DM values, refines ToA residuals, and generates diagnostic plots. The final outputs include DMX and DMMODEL ephemeris files, DM time series, and ToAs of high-SNR epochs.

The results of this work was presented as a poster at a workshop organized by SKA-Japan at National Astronomical Observatory of Japan, Tokyo.

The scope of the noise analysis has been expanded to incorporate this dataset. Notable improvements were made to the analysis methodology, including the simultaneous estimation of noise models and their harmonic modes. This enhancement addresses a limitation of the earlier serial implementation, which resulted in noise power leakage across different models.



3. Research plan for the next fiscal year

The research plan for the upcoming year involves applying the aforementioned methods to the InPTA DR2 dataset to search for potential signatures of the Gravitational Wave Background (GWB) within the data. The findings from this analysis will contribute to the broader International Pulsar Timing Array (IPTA) analysis.

4. List of awards, grants, and patents


None

5. List of journal papers in international journal as of the end of December; (excluding conference papers and proceedings)

Improving DM estimates using low-frequency scatter-broadening estimates, **Monthly Notices of the Royal Astronomical Society**, Volume 535, Issue 1, November 2024, Pages 1184–1192, <https://doi.org/10.1093/mnras/stae2405>

Comparing Recent Pulsar Timing Array Results on the Nanohertz Stochastic Gravitational-wave Background, **The Astrophysical Journal**, Volume 966, Issue 1, id.105 (2024)
<https://doi.org/10.3847/1538-4357/ad36be>

Low-frequency pulse-jitter measurement with the uGMRT I: PSR J0437–4715, **Publications of the Astronomical Society of Australia**, Volume 41, article id. e036, 05/2024
<https://doi.org/10.1017/pasa.2024.30>

No. 2-3-4	Seismic Performance and Evaluation of Hybrid Frame with CFST column continuous Beam Joints			
Name	Prafulla Bahadur MALLA	Title	Postdoctoral Researcher	
Affiliation	IROAST (-2025/2/28) Email: malla@kumamoto-u.ac.jp			
Research Field	Strengthening resilience			

[Details of activities]

The experimental work has been on progress to study the continuous beam type joint at the panel zone within a concrete filled steel tube (CFST) column. The experiment has been carried out on single bay frame (Figure 1). Three specimens have been prepared in which two specimens are continuous H-beam within CFST column (Figure 2) differing on axial load and the third one is with reduced section of flanges of H-beam (Figure 3) convenient concreting purpose in CFST column. The specimen has been subjected to large repetition of half cyclic loading. The large repetition of loading 290 repetition for 2% drift has been carried to understand the stiffness degradation under large repeated loading. The photograph from the experiment work has been shown in Photo1 with the load-drift curve in Figure 1. The loading on two specimens had been conducted and the loading on last specimen is on progress. The failure is primarily due to buckling of flanges of H-beam outside the panel zone (Photo 2) and buckling of steel tube of CFST column (Photo 3).

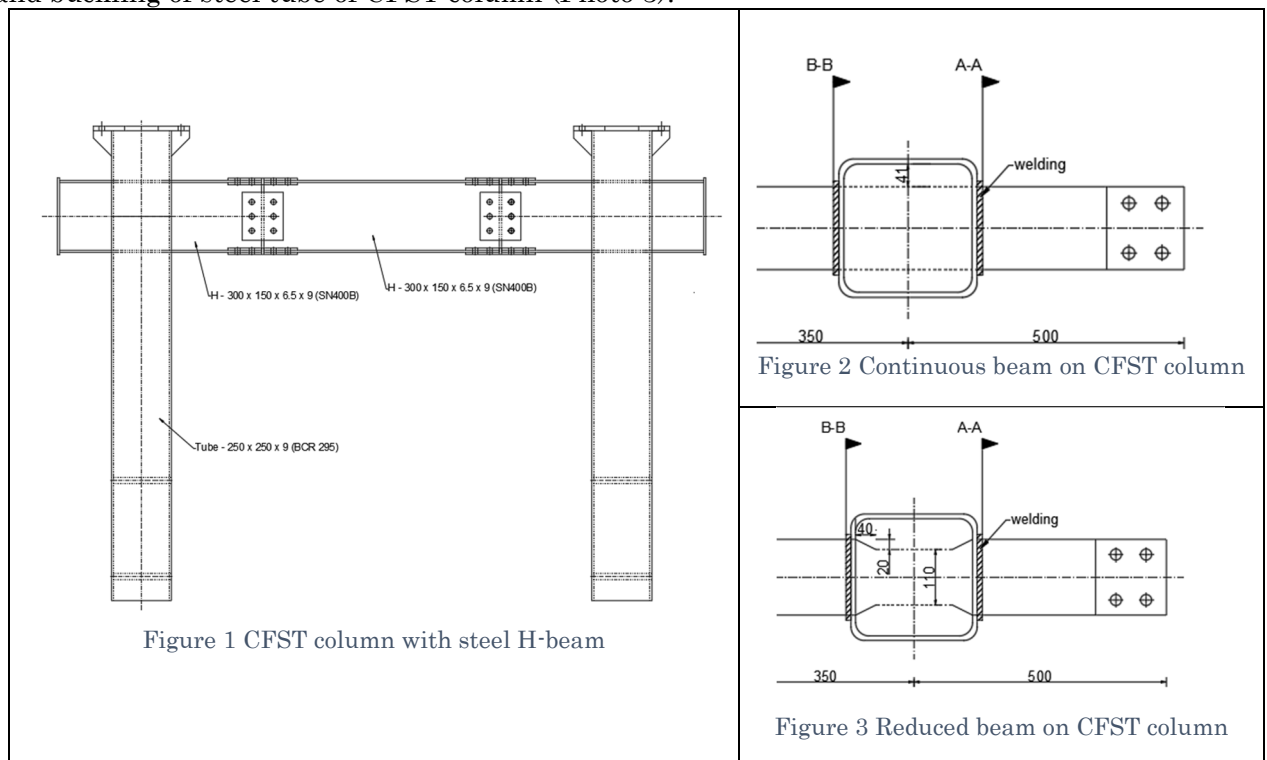




Photo 1 Experiment of CFST column with steel beam

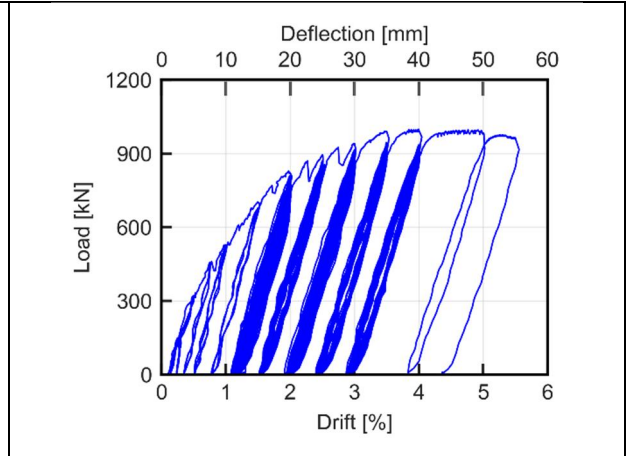


Figure 1: Load-drift curve from the experiment

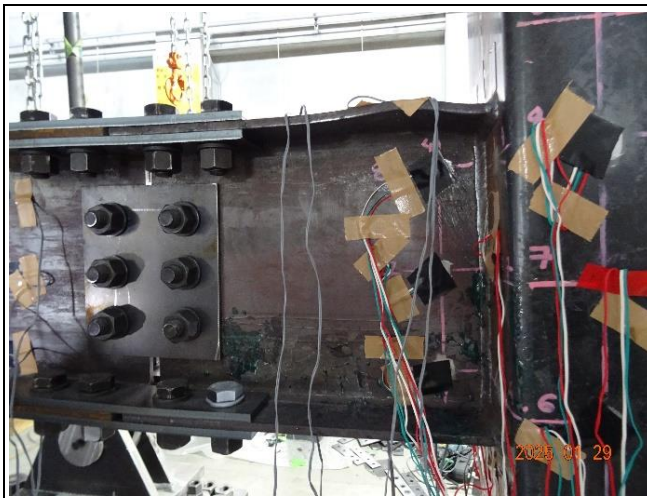


Photo 2 Buckling of beam flanges

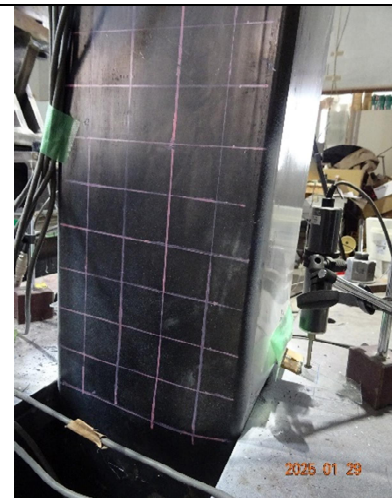



Photo 3 Buckling of steel tube on CFST column

2. List of journal papers in international journal as of the end of December; (excluding conference papers and proceedings)

1. Yue Wen, Gaochuang Cai, **Prafulla Bahadur Malla**, Hayato Kikuchi, and Cheng Xie. "Seismic Behavior of Resilient Reinforced Concrete Columns with Ultra-High-Strength Rebars Under Strong Earthquake-Induced Multiple Reversed Cyclic Loading." *Buildings* 2024, 14(12), 3747.

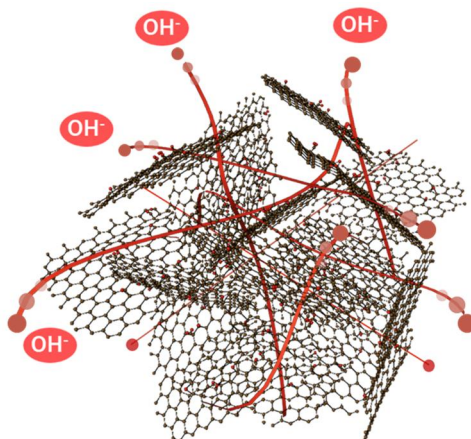
2. Wen, Yue, Gaochuang Cai, and **Prafulla Malla**. "Experimental and Transformer-Based Study on Seismic Behavior and Plastic Hinge Length of RC Columns Reinforced with End-Fixed Ultra-High Strength Rebars." *Buildings* 14.10 (2024): 3046.

3. Cai, G., Wen, Y., **Malla, P. B.**, Fujinaga, T., & Si Larbi, A. "Effect of axial load and shear span on seismic performance of CFT columns reinforced with end-fixed ultra-high strength rebars." *Bulletin of Earthquake Engineering* 22(9) (2024): 4515-4543.

No. 2-3-5	Oxide nanosheet as electrolyte for application in fuel cell			
Name	Mohammad Atiqur RAHMAN	Title	Postdoctoral Researcher	
Affiliation	IROAST Email: atiqur@kumamoto-u.ac.jp			
Research Field	Advanced materials			

1. Research outline and its perspective

This work focuses on fabricating three-dimensional alkaline graphene oxide (3DGO11) using a facile freeze-drying method for an efficient OH^- conductor. Compared to the 2DGO11, the current approach of 3DGO11 through a freeze-drying route ensures high porosity, enabling ion conduction in multiple directions with shorter pathways. The increased surface area and porosity facilitate high water absorption, ultimately leading to elevated hydroxide ion conductivity. Our study contributes to the advancement of graphene oxide applications in electrochemical energy conversion devices, offering a promising alternative to conventional fabrication methods.



Scheme: OH^- ion conductivity using three-dimensional alkaline graphene oxide

2. Research progress and results in the fiscal year

[Published] Graphite oxide was obtained by using a modified Hummers' method. Alkaline graphene oxide was prepared by adjusting the pH of the graphene oxide dispersion to pH = 11 using a dilute ammonia solution. For 2D alkaline GO (2DGO11), the as-prepared alkaline GO dispersion was vacuum filtered under reduced pressure using a membrane filter with a pore size of 0.45 μm followed by drying under ambient conditions. For three-dimensional alkaline GO (3DGO11), the dispersed alkaline GO solution was freeze-dried (FD-1000, EYELA) for 3 days. Finally, a pellet of 3DGO11 was fabricated using a pressure of 10 MPa. The ionic conductivity was evaluated for both in-plane and out-of-plane direction. The current study successfully demonstrates the fabrication of a three-dimensional alkaline graphene oxide membrane (3DGO11) through a facile freeze-dry method. The resulting membrane exhibits exceptional in-plane and through-plane OH^- conductivity, marking a substantial advancement in alkaline graphene oxide electrolytes. Notably, the 3DGO11 membrane achieves an outstanding 40-fold increase in ion conductivity in the through-plane direction compared to a 2D alkaline graphene oxide membrane. In the in-plane direction, the OH^- conductivity of 3DGO11 surpasses that of its 2D counterpart by a factor of 10. These remarkable conductivity

improvements underscore the three-dimensional structure's effectiveness in promoting ion transport, providing a substantial advantage over traditional two-dimensional membranes. The conductivity values of 2DGO11 and 3DGO11 were evaluated at 90% RH while adjusting the temperature, for in-plane and through-plane, respectively. The calculated activation energies for the in-plane direction were 0.19 eV and 0.09 eV for 2DGO11 and 3DGO11, respectively. Conversely, the E_a values in the through-plane directions were 0.18 and 0.10 eV for 2DGO11 and 3DGO11, respectively. These values suggest that the Grotthuss mechanism is responsible for hydroxide ion transfer. Furthermore, the type of ionic conduction was conducted by assessing the electromotive force (EMF). The EMF's sign serves as a crucial indicator to comprehend the type of ion conduction taking place in the respective membrane. Typically, a positive EMF signifies cationic conduction, while anionic conductors exhibit a

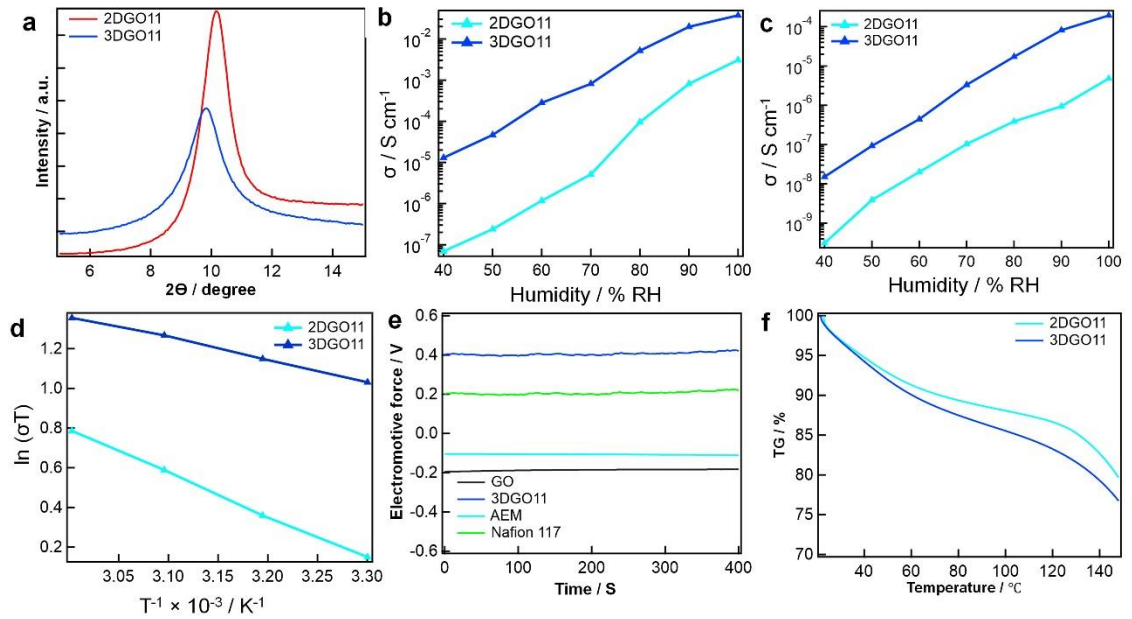


Figure: (a) PXRD pattern of 2DGO11 and 3DGO11; (b) Humidity dependent OH⁻ conductivity: (b) In-plane and (c) Through-plane direction measured maintaining several humidified conditions at 25 °C; (d) Arrhenius plots of ln(σT) vs. T^{-1} for in plane pathways; (e) Identification of the type of ion conduction: measurement of EMF value using water vapor concentration cell using Nafion; (f) weight loss profiles were discovered using TGA analysis in an N₂ environment for 2DGO11 and 3DGO11.

negative EMF. For comparison, incorporating 3DGO11 and AEM into the concentration cell resulted in a negative EMF value, contrasting with the positive EMF observed for GO and Nafion 117. This unmistakably indicates that the nature of ion conduction in 3DGO11 involves hydroxide ions. Furthermore, the outcomes of a thermogravimetric analysis (TGA) shows that there is a weight loss of 15% for 3DGO11, in contrast to the 12% weight loss observed for 2DGO11 when the materials are heated up to 100 °C. The amount of adsorbed water is of particular importance as it directly influences ionic (H⁺ or OH⁻) conductivity, a critical factor in fuel cell operation. Therefore, higher hydroxide ion conductivity of 3DGO11 in comparison to 2DGO11 may be due to higher water absorption capacity and porosity originated from the freeze-drying route which enable higher hydroxide conductivity.

3. Current research and future plan

Currently I am working on the design and fabrication of electrolyte based on metal oxide nanosheet. This includes the synthesis of doped and undoped calcium niobium oxide nanosheet. This synthesis includes, preparation of layered metal oxide using solid state reaction of K₂CO₃, CaCO₃ and Nb₂O₅ (ratio=1.3:2:3) followed by proton exchange and

delamination using tetrabutyl ammonium hydroxide (TBAOH). Membrane of these films was fabricated by vacuum filtration and ion exchange using hydrochloric acid.

I am focusing on focused on the following points:

- ❖ Synthesis and characterization of doped and un-doped calcium niobium oxide nanosheet.
- ❖ Effect of Mg-doping on the proton conductivity and proton exchange membrane fuel cell performance of calcium niobium oxide nanosheet.
- ❖ Effect of proton concentration on the proton conductivity and proton exchange membrane fuel cell performance of calcium niobium oxide nanosheet.
- ❖ LDH nanosheet membrane as electrolyte for application in proton exchange membrane fuel cell.
- ❖ Finally, this project will lead towards the achievement of carbon neutral society for achieving the SDGs.

4. List of journal papers (with IROAST as your affiliation) published between April 2024 and March 2025.

- [1]. Effect of proton concentration on the proton conductivity of calcium niobium oxide nanosheet, M. A. Rahman, K. Hatakeyama, and S. Ida* (*Manuscript under preparation*).
- [2]. Electrokinetics of CO₂ reduction in imidazole medium using RuO₂.SnO₂ immobilized glassy carbon electrode, M. Rahman, M. F. Islam, M. M. Hossain, M. N. Islam, M. M. Hasan, M. A. Rahman, Z. M. Moushummy, N. A. T. A. Tanjila, M. A. Hasnat,* *Molecules (Under review)*.
- [3]. Activation of stannic oxide by the incorporation of ruthenium oxide nanoparticles for efficient hydrogen evolution reaction, M. N. Islam, Z. M. Moushummy, M. R. Islam, M. I. Hossain, M. A. Rahman, M. Rahman, A. Aldalbahi, M. T. Uddin, N. R. Singha, M. A. Hasnat,* *Electrochimica Acta*, 507, 2024, 145114.
- [4]. Engineering Zeolitic-Imidazolate-Framework-Derived Mo-Doped Cobalt Phosphide for Efficient OER Catalysts, M. A. Rahman, Z. Cai, Z. M. Moushummy, R. Tagawa, Y. Hidaka, C. Nakano, M. S. Islam, Y. Sekine, Y. Nishina, S. Ida, and S. Hayami,* *ACS Omega*, 9 (34), 36114–36121, 2024 .
- [5]. Enhanced OH[−] conductivity from 3D alkaline graphene oxide electrolytes for anion exchange membrane fuel cells, Nonoka Goto, M. A. Rahman, M. S. Islam, R. Tagawa, C. Nakano, M. S. Ahmed, Y. Sekine, Y. Nishina, S. Ida, and S. Hayami,* *Energy Advances*, 3(5), 1047-1053, 2024.
- [6]. Ce-doped TiO₂ fabricated glassy carbon electrode for efficient hydrogen evolution reaction in acidic medium, M. N. Islam, M. M. Hossain, S. S. Maktedar,* M. Rahaman, M. A. Rahman, M. A. Hasnat*, *Chemistry—An Asian Journal*, 19(16), e202301143, 2024.

5. List of awards, grants and patents

- None

6. Other activities

- [Participation in conference]

- a. "Calcium Niobium Oxide Nanosheet for Application in Proton Exchange Membrane Fuel Cell"; **M. A. Rahman**, K. Hatakeyama and S. Ida, *E-MRS Spring Meeting 2024*, Stasbourg, France, May 27-31, 2024.
- b. Engineering Zeolitic Imidazolate Framework Derived Mo-Doped Cobalt Phosphide for Efficient OER Catalysts, **M. A. Rahman**, K. Hatakeyama and S. Ida, *18th ICC 2024*, Lyon, France, July 14-19, 2024.



Fig. 1 ICC-Lyon 2024

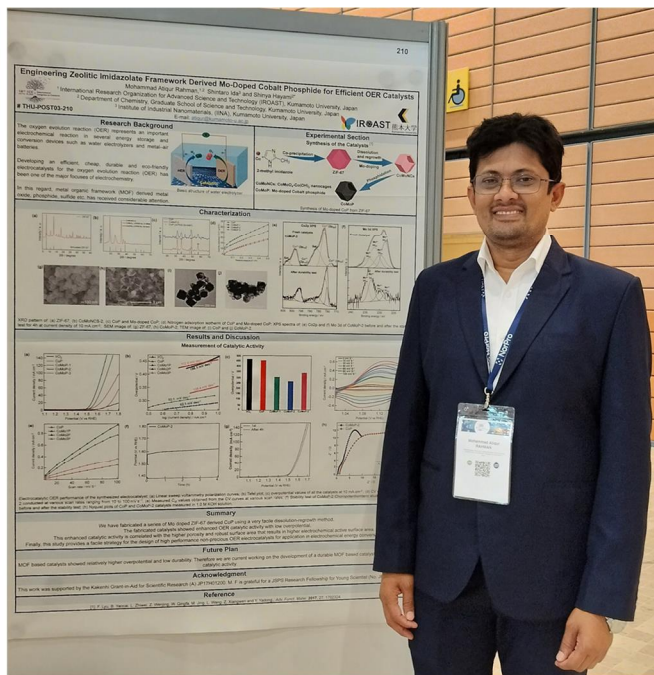



Fig. 2 ICC-Lyon 2024

No. 2-3-6	Applications of Functional Materials in Environmental Remediation			
Name	Reetu Rani	Title	Postdoctoral Researcher	
Affiliation	IROAST Email: ranireetu@kumamoto-u.ac.jp			
Research Field	Environment-friendly technology			

[Details of activities]

1. Research outline and its perspective

At even trace levels, certain ionic solutes pose significant challenges to human health, the environment, and various industrial applications, including semiconductors. As a result, there is a great need for methods to separate targeted solutes from complex matrix samples, such as seawater, commercial chemicals, and wastewater. This necessitates the development of materials that exhibit exceptional extraction and adsorption capabilities for these solutes. Metal organic frameworks (MOFs), which are porous crystalline materials made up of organic and inorganic units, are considered promising materials for environmental remediation applications due to their high surface area, tunable pore size, ease of functionalization, and high stability. Additionally, Molecularly Imprinted Polymers (MIPs), another class of advanced materials, offer selective adsorption capabilities for specific target molecules, further enhancing their role in environmental remediation strategies.

2. Research progress and results in the fiscal year

a) **Utilizing zirconium-based metal-organic framework (Zr-MOF) for water remediation applications:** In FY 22 and FY 23, adsorptive behavior of carboxyl group-functionalized Zr-MOF (UiO-66-(COOH)₂) was investigated for adsorption of alkali and alkaline earth metal ions from multielement aqueous solutions. UiO-66-(COOH)₂ showed significant adsorption capacity towards divalent metal ions (Fig. 1). Further, a thorough investigation was conducted to understand how pH, initial concentration, and MOF dosage impact the adsorption properties of UiO-66-(COOH)₂. At the natural pH of the solution, UiO-66-(COOH)₂ exhibited a superior adsorption capacity towards Sr²⁺ (15.3 mg g⁻¹), and Ca²⁺ (7.9 mg g⁻¹). Linear and non-linear pseudo first order (PFO) and pseudo second order (PSO) kinetic models were fitted to adsorption data to elucidate the mechanisms involved in adsorption of Ca²⁺ and Sr²⁺ on Zr-MOF. Linear and non-linear PSO model showed good fitting for the divalent ions indicating chemisorption was the rate determining step. Additionally, the adsorption behavior of UiO-66-(COOH)₂ for 24 elements was evaluated, and the MOF showed significant adsorption of Sr²⁺ and Ca²⁺ along with other divalent and trivalent metal ions. The experimental findings of the present study suggest that carboxylic-functionalized Zr-MOF holds significant potential towards the preparation of suitable sorbents for extraction of higher valence metal ions. The results of this study are published in *Bulletin of the Chemical Society of Japan*.

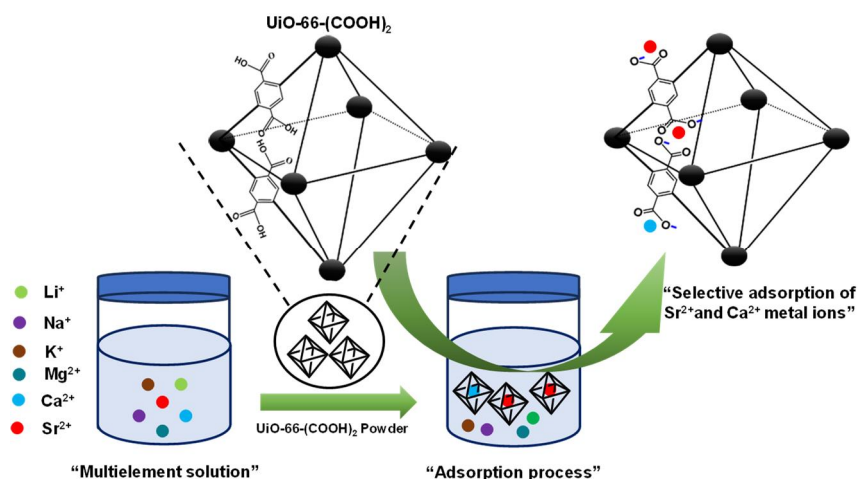


Fig. 1: Schematic showing adsorption of metal ions on UiO-66-(COOH)₂ from a multielement metal ion solution.

- b) **Synthesis of molecularly imprinted polymer for urea adsorption:** In FY 2024, I am working on molecularly imprinted polymer/ membranes (MIP/MIM) for adsorption of urea. For this, I have prepared a MIP based on methacrylic acid-based monomer. The adsorptive behavior of the synthesized MIP was tested in a urea solution and a traditional DAMO-TSC method was used to test concentration of urea before and after adsorption calorimetrically. As shown in the Fig. 2, color intensity of the solution decreased after adsorption, compared to the urea sample solution, indicating adsorption of urea onto the MIP. Future studies will focus on optimizing the synthesis and adsorption process parameters to enhance the performance of urea-MIP.

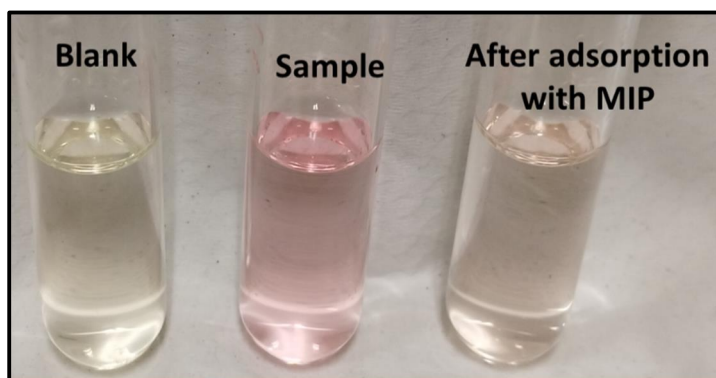


Fig. 2: Colorimetric detection of urea in blank, urea sample before adsorption and urea sample after adsorption with MIP.

3. Research plan for the future

Imprinted polymers/ membranes will be tested for their efficiency in removing urea from solutions. This will involve optimizing the synthesis of MIPs/MIMs and adjusting adsorption parameters to enhance their overall performance.

4. List of journal papers (with IROAST as your affiliation) published between April 2024 and March 2025.

Journal Papers:

- a) R. Rani, T. Ueda, K. Saeki, K. Toda, S-I. Ohira, Adsorption behavior of zirconium metal-

- organic frameworks in multicomponent metal-ion solutions, *Bulletin of the Chemical Society of Japan*, 97, uoae113 (2024), <https://doi.org/10.1093/bulcsj/uoae113>.
- b) M. Mukai, R. Rani, N. Iwanaga, K. Saeki, K. Toda, S-I. Ohira, Two-step extraction for the evaluation of metal–organic framework impregnated materials, *Analytical Sciences*, 40, 1793-1797 (2024), <https://doi.org/10.1007/s44211-024-00608-5>.
- c) B. B. Sherpa, R. Rani, Advancements in explosive welding process for bimetallic material joining: A review, *Journal of Alloys and Metallurgical Systems*, 6, 100078 (2024), <https://doi.org/10.1016/j.jalmes.2024.100078>.

Book Chapter:

- a) R. Rani, M.E. Jinugu, P. Gangwar, P. Thareja, A. Parihar, M. Garg, Lab-on-a-chip: A Novel Platform for Disease Diagnosis, *Royal Society of Chemistry (RSC)*, 25, 695, 158 - 189 (2024). <https://doi.org/10.1039/9781837673476-00158>.